JOURNAL OF SPACECRAFT AND ROCKETS
Vol. 33, No. 2, March–April 1996

Microencapsulated Phase-Change Material Suspensions for Heat Transfer in Spacecraft Thermal Systems

J. C. Mulligan*
North Carolina State University, Raleigh, North Carolina 27695-7910
and
D. P. Colvin† and Y. G. Bryant‡
Triangle Research and Development Corporation, Research Triangle Park, North Carolina 27709-2696

The potential for improvement of liquid-coupled heat exchange by utilizing a two-component suspension consisting of a carrier fluid and a microencapsulated phase-change material is presented. A system analysis utilizing a water suspension shows the effects on system behavior. Enhancement of fluid heat capacity and heat transfer coefficient is shown, along with reductions of system temperatures. Results of experiments are presented in which 10–30-μm particles of various microencapsulated paraffins were slurried with water as well as silicone oil and circulated in a model heat exchange loop. Enhancement of heat transfer coefficients and thermal properties, and reductions in system temperatures, are shown to occur experimentally. Significant improvements in overall performance are shown to be achievable.

Nomenclature

A	= heat transfer surface area, m^2
c	= specific heat, kJ/kg · °C
$\bar{c}$	= average sensible specific heat, kJ/kg · °C
D	= heat-exchanger diameter, m
F	= fraction of phase-change material (PCM) in suspension that is actively changing phase, $f_1 - f_2$
F^*	= fraction of PCM in suspension
f	= fraction of PCM in suspension that is solid
h_i, h_o, h_S	= heat transfer coefficient on inside and outside of rejection tube and on heating source, W/m^2 ·°C
k	= thermal conductivity, W/m ·°C
L	= heat-exchanger length, m
$\dot{m}$	= mass flow rate, kg/s
Nu	= Nusselt number based on diameter
P	= pumping power, kW
Pr	= Prandtl number
$\dot{Q}_{\text{in}}$	= source heating rate, W
Re	= Reynolds number based on diameter
r	= heat-exchanger radius, m
T	= source temperature, °C
T_{ci}	= coolant inlet temperature, °C
T_m	= melting–freezing temperature of PCM, °C
T_{S2}	= temperature of source near flow outlet, °C
U	= overall heat transfer coefficient, W/m^2 ·°C
V	= average flow velocity, m/s
α	= particle volume fraction
ΔP	= pressure drop, N/m^2
ΔT	= system overall temperature difference $T_{S2} - T_{ci}$, °C
ΔT_{TOT}	= temperature change, °C
ε_R	= effectiveness of rejection heat exchanger
λ	= particle latent heat, kJ/kg
μ	= absolute viscosity, kg/m · s
ρ	= suspension density, kg/m^3

Subscripts

c, f, s, S, w	= coolant, working fluid, suspension, source, water
PCM	= PCM capsule
1,2	= suspension inlet and outlet states

Presented as Paper 94-2004 at the AIAA/ASME 6th Joint Thermophysics and Heat Transfer Conference, Colorado Springs, CO, June 20–23, 1994; received Nov. 28, 1994; revision received April 28, 1995; accepted for publication May 12, 1995.

*Professor, Department of Mechanical and Aerospace Engineering.
†President, P.O. Box 12696. Member AIAA.
‡Senior Research Chemist.

Introduction

PHASE-CHANGE materials (PCMs) have long been used as thermal control materials because of the heat absorption and release that occurs upon change of phase, with little attendant change in temperature. Materials that undergo solid–liquid transition have been investigated for a variety of thermal control applications in space as well as terrestrial applications. In the late 1970s, an effort was made to enhance the energy storage capability of structural materials for terrestrial applications by incorporating PCMs directly within materials.[1] Along with this effort, a new approach was introduced[2] incorporating microencapsulated PCMs (MEPCMs) directly into a heat transfer fluid (i.e., as a particle–liquid suspension) to enhance both its heat transfer characteristics and its energy storage characteristics. By microencapsulating the PCM, the core material is always separated from the carrier fluid, preventing its deposition within the system. Various companies were enlisted to microencapsulate the PCMs, and tests of the suspensions were carried out. The use of fluidized particles to enhance heat transfer in space cooling systems was not new,[3] but the use of microscopic particles that are encapsulated liquids under warm conditions and encapsulated solids under cooler conditions was very new. This original program was not successful, however, because of the lack of strength and structural integrity of the small MEPCM capsules. Gradually, interest in the technique has revived. In 1982, an effort was made to manufacture microencapsulated PCM particles of greater strength,[4] and the reported results were promising. In 1984, an analytical estimate of the merits of this fluidized suspension technique in solar energy systems was presented by Kasza and Chen.[5] More recently, a numerical analysis of some of the heat transfer characteristics of such suspensions was presented by Charunyakorn et al.[6]

The potential use of microencapsulated PCMs in various thermal control applications is limited to some extent by their cost. However, because the performance of thermal control for space applications is so important and because costs are less important, it is believed that the development of such PCMs could be a milestone for space technology. Some of the potential benefits of microencapsulated PCMs in space applications have been discussed in the literature.[7–9] New developments in the thermal management of spacecraft systems are of interest because of significant increases in the intensity

and periodicity of thermal loads, and the growing need to minimize system weight and volume. Heating and cooling systems must be sized to accommodate peak loads and thus usually have considerable idle capacity for much of the time. Moreover, future spacecraft can be expected to utilize a greater variety of power systems, which require cooling for various mission applications. Many electronic instruments, including computer, radar, and avionic components, are notably sensitive to temperature variations and thus could benefit from advanced means of temperature control. In addition to the benefits of controlling temperature at the source, it is also useful to attempt to utilize smaller heat rejection systems, utilizing smaller volumes of working fluid and requiring less power, thus saving considerably on the size and weight of these components.

This paper presents the results of a study of liquid-coupled heat exchange incorporating an MEPCM suspension as the working fluid. An analytical system model is first presented to show the benefits and performance that such a fluid might provide. Experiments are then described that actually used such a thermally enhanced fluid in a model liquid-coupled heat exchange loop.

Analysis

An illustration of an MEPCM particle (approximately 83% core and 17% wall) and a typical liquid-coupled heat-exchanger system is shown schematically in Fig. 1. The heat source is represented by a simple tubular heat exchanger, which is heated electrically at its outer surface with a constant and uniform heat flux. After the working fluid (carrier fluid or suspension) absorbs heat, it is pumped through a rejection heat exchanger, giving up heat to a secondary fluid. In the analysis it is assumed that $T_{f2} = T_{f3}$, $T_{f1} = T_{f4}$, and $T_{f2} > T_{f1}$. The fraction of the MEPCM that is solid in the suspension is designated as f. Hence, the solid fraction of PCM on entering the heat source is f_1, and on leaving f_2. The fraction of PCM that is active is $F = f_1 - f_2$ and is variable, whereas the fraction that is loaded is F^* and is a constant. During the phase change process the small microcapsules will expand slightly during melting and contract slightly during freezing, usually on the order of 10%. A dimple can even appear if the microcapsule is initially formed as a liquid, and wall cracking and failure can occur if the microcapsule is initially formed as a solid and the wall is too thin and too inflexible. The size of the capsules (10–30 μm) and their small difference in density ensures that they effectively move isokinetically at the Reynolds numbers of a forced-flow stream, causing no significant microconvective effects because of relative motion between capsule and carrier fluid.[10] Additionally, because of their very large surface-to-volume ratio, it is realistic to expect them to change phase very quickly in comparison with the component residence time, and hence, not to introduce phase-kinetic considerations.

The rejection heat exchanger is taken to be a standard shell-and-tube (double-pipe) counterflow heat exchanger with the working fluid occupying the inner tube and a secondary coolant fluid circulated through the shell. The energy balances, heat transfer, and pumping requirements for the working fluid are modeled as follows:

$$\frac{\dot{Q}_{\text{in}}}{\bar{c}(\Delta T)_f + F\lambda} = \dot{m}_f \tag{1}$$

$$P = \dot{m}_f(\Delta P)/\rho_f \tag{2}$$

$$\Delta P = 4C_B \frac{L}{D}\frac{\rho_f V^2}{2} \tag{3}$$

$$C_B = \begin{cases} 0.046\,Re^{-0.2} & \text{for turbulent flow} \\ 16/Re & \text{for laminar flow} \end{cases} \tag{4}$$

Heat dissipation through the rejection heat exchanger is formulated, using the effectiveness of the unit ε_R, as

$$\dot{m}_f\left[\bar{c} + \frac{F\lambda}{(\Delta T)_f}\right](\Delta T)_f = \varepsilon_R(T_{f2} - T_{ci})\dot{m}_c c_c$$

$$= \varepsilon_R[(T_{S2} - T_{ci}) - (T_{S2} - T_{f2})](\dot{m}_c c_c) \tag{5}$$

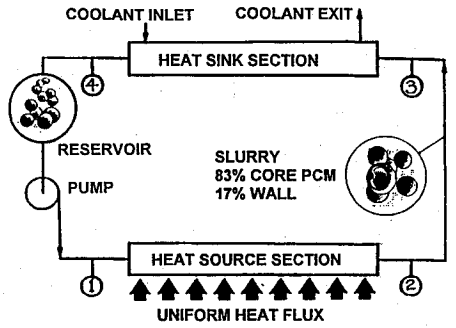

Fig. 1 Schematic of liquid-coupled heat exchange system used for both simulation and experiments.

For the heating element, it is assumed that $\dot{Q}_{\text{in}}$ = constant and the fluid flow is fully developed. Thus, the heat transfer coefficient h_S is assumed to be constant and

$$\frac{\dot{Q}_{\text{in}}}{2\pi r_S L_S} = h_S(T_{S2} - T_{f2}) \tag{6}$$

Substituting Eq. (6) into Eq. (5) and noting that $T_{S2} - T_{ci} = (\Delta T)_{\text{TOT}}$ yields

$$(\Delta T)_{\text{TOT}} = \frac{\dot{m}_f[\bar{c} + F\lambda/(\Delta T)_f](\Delta T)_f}{(\dot{m}_c c_c)\varepsilon_R} + \frac{\dot{Q}_{\text{in}}}{2\pi r_S L_S h_S} \tag{7}$$

which is simply a statement that $(\Delta T)_{\text{TOT}} = (\Delta T)_R + (\Delta T)_S$, for the rejection and source units. The effectiveness is assumed to be represented by the usual expression

$$\varepsilon_R = \frac{1 - \exp[(-UA/C_{\min})(1 - C_{\min}/C_{\max})]}{1 - (C_{\min}/C_{\max})\exp[(-UA/C_{\min})(1 - C_{\min}/C_{\max})]} \tag{8}$$

where $C_{\max} = \dot{m}_c c_c$, $C_{\min} = \dot{m}_f[\bar{c} + F\lambda/(\Delta T)_f]$, or vice versa, as appropriate.

The overall heat transfer coefficient for the rejection heat exchanger, neglecting conductive resistance in the thin-walled copper tube and assuming equal surface areas, is

$$U = \frac{1}{1/h_i + 1/h_o} \tag{9}$$

If the flow is turbulent, the heat transfer coefficients for the double-pipe rejection heat exchanger and the heat transfer coefficient for the heating source can be calculated from the Petukhov expression

$$Nu = \frac{Re\,Pr(C_B)/2}{1.07 + 12.7\left(Pr^{\frac{2}{3}} - 1\right)C_B/2} \tag{10}$$

If the flow is laminar, the heat exchangers cannot be assumed to be fully developed. Accordingly, Nu is approximated by

$$Nu = \frac{3.66 + 0.0668(X^+)^{-1}}{1 + 0.04(X^+)^{-\frac{2}{3}}} \tag{11}$$

$$X^+ = \frac{L}{D\,Re\,Pr} \tag{12}$$

Appropriate corrections are made for the annulus flow.

The heat transfer modeling expressed by the equations is entirely appropriate for purely sensible-heat working fluids as long as the properties are evaluated at the proper temperature states. However, for an MEPCM suspension it is not at all clear how the heat transfer coefficients should be determined, or how these known relationships can be applied to such a fluid. Sohn and Chen[10] have shown that in the particle size range of interest, fluid microconvection and particle-to-particle interaction effects have little significance. Watkins et al.[11] suggest that in suspension flows, segregation occurs and a pure-fluid layer develops adjacent to surfaces, which controls the heat transfer. However, with the small particle size and neutral buoyancy of

Table 1 Sample calculations of c_s for typical values of $\bar{c}$ (3.56 kJ/kg ·°C), F (0.3), and λ (210 kJ/kg)

$(\Delta T)_S$, °C	c_s, kJ/kg ·°C
1.5	45.56
2.5	28.76
5.0	16.16

the present application, it is difficult to believe this is a significant mechanism. Our approach is to assume that the suspension essentially behaves as a uniform continuum with effective properties that incorporate latent-heat effects. Hence, the same formulation is assumed to apply, except that the specific heat and Prandtl number are calculated utilizing F and $(\Delta T)_S$. That is, the effective specific heat is used instead of the weighted average. Enhancement of heat transfer is therefore believed to be essentially a Pr effect (entry-region effect) caused by latent enthalpy. An example of the potential magnitude of the effective specific heat is illustrated in Table 1.

A significant enhancement of thermal performance potentially can be achieved by properly designing the operating temperature to take advantage of the phase-change thermal energy storage. In the calculations, it is assumed that the PCM melts at a fixed temperature and requires no supercooling, and that the capsules are sufficiently small to melt essentially instantaneously. The latter assumption means that their residence times in the heat exchangers are sufficiently large so that the amount of the PCM appropriate for the system flow rate, heat rate, and temperatures (i.e., the value of F for the system conditions) is utilized. The definitions of $\bar{c}$, c_s, and the suspension density ρ are

$$\bar{c} = c_w(1 - F^*) + F^* c_{\text{PCM}} \tag{13}$$

$$c_s = \bar{c} + F\lambda/(\Delta T)_f \tag{14}$$

$$\rho_s^{-1} = \rho_w^{-1}(1 - F^*) + F^* \rho_{\text{PCM}}^{-1} \tag{15}$$

The suspension viscosity is an important parameter in that it influences directly the tradeoff between thermal performance and pumping power. For sufficiently high-concentration suspensions of small-diameter spherical particulates, Vand[12] gives the viscosity as

$$\mu_s = \mu_f(1 - \alpha - B\alpha^2)^{-2.5} \tag{16}$$

Here $B = 3.4$ (obtained experimentally) and α is the particle volume fraction. This relationship is fairly independent of particle size in the 3- to 300-μm range. The assumption of Newtonian behavior of the PCM suspension in the present case is based on the nearly spherical shape of the PCM particles and is also important for the overall behavior of the suspension. Because the apparent viscosity of the suspension is almost three times that of water, most applications will involve laminar flow. Therefore, for the calculations in this paper the suspension was assumed to be in laminar flow throughout the system.

The effective thermal conductivity k_s of the suspension is a much more difficult quantity to determine, because very little information is available in the literature. It is known that its value depends both upon the mass fraction of the suspension that is particulate material and upon the particle size and shape. For spherical particles Torquato[13] provides the relation

$$k_s = k_w\left(\frac{1 + C_1\beta + C_2\beta^2}{1 + d_1\beta + d_2\beta^2}\right), \qquad \text{where} \quad \beta = \frac{k_{\text{PCM}} - k_w}{k_{\text{PCM}} + 2k_w} \tag{17}$$

and the constants C and d are experimentally determined. When the k values are very close, this expression suggests $\beta \approx 0$ and $k_s \approx k_w \approx k_{\text{PCM}}$. Also, when individual k values are not as close but still of the same order, k_s is well approximated by a weighted average, which is essentially the case in the present work.

Equations (1–17) are difficult to solve because of the unknown value of F. This parameter is required to evaluate the effective suspension properties c_s and Pr_s, but itself requires these properties for its own determination. Hence, it is part of the solution. An iterative procedure was utilized that determines T_{f1}, T_{f2}, f_1, and f_2 by repeated calculations until convergence, and hence determines F, c_s, h_S, and other parameters for each set of conditions of coolant flow rate, coolant temperature, suspension flow rate, and system input heat rate. If T_{f2} turns out to be less than the melting temperature T_m for given conditions, then all the PCM will be solid and F will be zero. If T_{f2} turns out to be greater than T_m, then F will have a value between zero and F^*, depending on the conditions. If T_{f1} is greater than T_m, then clearly F will be zero and all the PCM will be liquid throughout the system. If conditions are such that $T_{f2} \approx T_{f1}$ and $F \approx F^*$, then the system is tuned to the minimum ΔT_f and the maximum utilization of the PCM. A variety of conditions were specified and this tuning behavior of the system was studied. Results for F, $(\Delta T)_f$, h_S, and c_s were developed to illustrate this thermal behavior of a liquid-coupled system utilizing an MEPCM fluid suspension.

Experiments

A liquid-coupled heat exchange loop consisting of heat exchangers, piping, pump, reservoir, and instrumentation similar to the schematic of Fig. 1 was utilized as the experimental apparatus. A heat source consisting of a custom-wound electrical heating element, externally insulated, on a 1.1-m-long (6.1-mm i.d., 0.75-mm wall) straight copper tube was used. Type T (copper–constantan) thermocouples were equally spaced along the tube wall at seven locations, and in the inlet and exit flow streams. The heat sink consisted of a double-pipe copper heat exchanger with the internal tube used for the working fluid and the shell-side tube used for the coolant flow (water). The inside tube was 0.91 m long and made of the same 6.1-mm-i.d. (0.75-mm-wall) tubing. The outer tube was a 0.0222-m-i.d. copper tube of the same length. Inlet and outlet temperatures and flow rates were measured. The flow through the heat exchanger was counterflow, and the unit was well insulated.

The PCMs used in the study were n-octadecane, n-eicosane, n-heptadecane, and n-nonadecane, combined with either water or silicone oil as the carrier fluid. The capsules were approximately 83% core material and 17% wall material. The wall was constructed of a polymer material by phase separation techniques, and the capsules were generally in the 10–30-μm range. During the course of the testing, various capsule concentrations were used, ranging from 4 to 32% by weight. These particular suspensions were selected for study because the nontoxic water-based medium is potentially applicable in spacecraft environmental systems, whereas the dielectric medium is useful for avionics systems. The component properties are listed in Table 2.

The liquid-coupled heat exchange system was tested with both water and silicone oil to determine a baseline mode of operation under various source heating rates and various flow rates. These data, along with analytical estimates, form the primary basis of comparison for the PCM suspension. To obtain a zero-heat-input condition, the heating element was first turned off and the system allowed to reach thermal equilibrium. At this point the water flow rate and the cooling-water flow rate were measured, various temperatures were

Table 2 Thermophysical properties of suspension components (liquid state) at 20°C, from manufacturer's data

Material	Temp., °C	ρ, kg/m^3	c, kJ/kg ·°C	k, W/m ·°C	λ, kJ/kg
Water[a]		998	4.18	0.60	NA
Silicone oil[a] (5 cS)		911	1.72	0.11	NA
Heptadecane	23	776	2.14	0.15	165
Octadecane	27	775	2.09	0.15	237
Nonadecane	32	784	2.09	0.15	191
Eicosane	37	787	2.09	0.15	239
Amino–formaldehyde		1327	1.67	0.14	NA

[a] $\mu = 993 \times 10^{-6}$ and 4.55×10^{-3} kg/m · s, for water and silicone oil, respectively.

recorded, and various pressures recorded. Then, without changing the flow rates, power was applied to the heating element, and the voltage and current recorded. When the system reached thermal equilibrium, all of the measurements were repeated. Equilibrium points corresponding to various levels of heating and various levels of pumping were recorded. In all of the tests, the cooling-water flow rate was maintained constant at or near 0.5 gal/min and the entering cooling temperature maintained constant at or near 20°C. Various quantities of interest in the study were calculated from these data.

In the suspension tests a magnetically coupled centrifugal pump was used to circulate the heat transfer fluid. The pump was a dc, five-speed device with a low rotational speed of 1020 rpm. This particular centrifugal pump (Lange model 200) was chosen because of its lower-than-typical speeds and its impeller design, which appeared as though it would be reasonably gentle with the suspension. The experiments began when approximately 1 liter of the suspension was mixed to the appearance of a uniform fluid with the prescribed percentage of PCM, and charged into the system. The small capsules were not visible to the naked eye, and the suspension appeared as a viscous fluid with a distinct color. The system was then run through a series of tests by altering the voltage levels on the heating element and allowing the system to reach thermal equilibrium. Temperatures and pressures were then recorded.

Results

The numerical simulation of the loop was carried out to demonstrate its behavior when utilizing the MEPCM suspension and to learn the ranges of the variables that are necessary to drive the loop through its tuning conditions. Results are presented for the case of a 21% mixture of heptadecane capsules in water (83% core and 17% wall) with approximately 17.5% PCM by weight. Figure 2 illustrates the typical behavior of the inlet and outlet temperatures as the heating rate to the loop is increased from approximately 10 to 100 W while all other system parameters are maintained constant. For this particular case the cooling-water flow rate and inlet temperature were 0.5 gal/min and 10°C, respectively, while the suspension flow rate was maintained at 0.0035 kg/s. As the heating rate is increased, the temperature of the working fluid increases until its hottest point, T_2, reaches the PCM melting temperature, at which time it tends to level off and remain constant as the heat rate is further increased. That is, the latent storage capacity of the MEPCM fluid becomes active, begins absorbing a larger portion of the heat as the heating rate is increased, and hence effectively controls the maximum loop temperature. The inlet temperature is seen to follow and eventually approach the melting point as the loop becomes optimally tuned to its minimum ΔT. As the inlet temperature approaches T_m (22.4°C), the exit temperature, at some value of the heating rate, begins increasing rapidly as the system starts becoming detuned to the hot side. The overlap region, wherein T_1 and T_2 are both close to T_m and before T_2 has begun its upward movement, is the tuning region of the loop.

This behavior was found to be characteristic for all sets of loop conditions, and is even more clearly demonstrated in Fig. 3. Here,

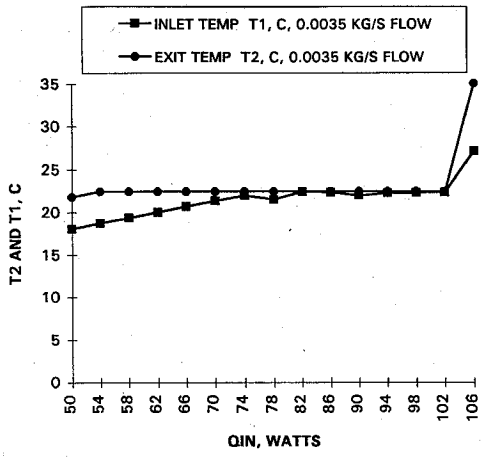

Fig. 2 Typical variation of system temperatures with applied heating rate.

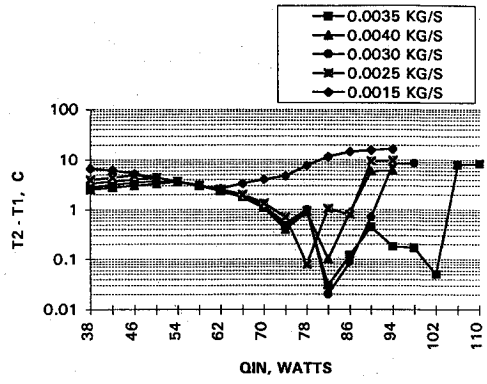

Fig. 3 Temperature rise across heater vs heating rate.

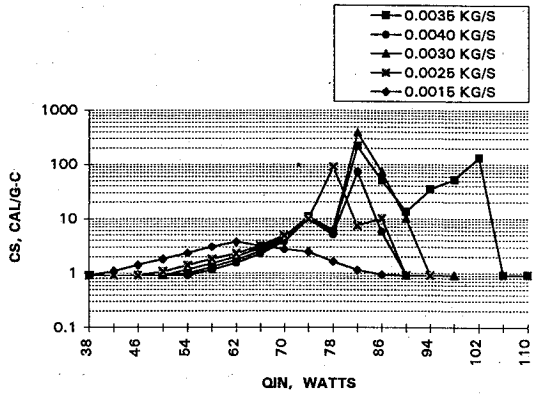

Fig. 4 Prediction of suspension effective specific heat as heating rate varies.

$\Delta T = T_2 - T_1$ for the loop is shown versus the system heating rate for the same conditions and various suspension flow rates. The tuning windows are clearly evident, and depend upon both flow rate and heating rate. The minimum ΔT is also seen to be different in each case. Similar results can be plotted by dividing the heating rate by the product of the system ΔT and the suspension flow rate. This quantity is therefore the suspension effective specific heat c_s and is plotted versus heating rate in Fig. 4.

This is perhaps one of the most important parameters, because it influences the fluid Prandtl number $\mu_s c_s / k_s$ and therefore indirectly influences the entry-region effect and the calculation of the suspension heat transfer coefficient. The effective specific heat of the suspension is seen to become very large as the loop enters the tuning window and the system ΔT becomes very small. That is, heat is being transferred primarily as latent heat. Again, as before, the maximum values of c_s within the tuning window depend upon the flow rate and heating rate, and are not necessarily all equal. The particular values reached by c_s in the tuning are significant primarily in indicating the proper combination of system conditions, heating rate, and flow rate for optimal operation.

The phase change fraction F is shown plotted versus the heating rate in Fig. 5, again for the same conditions and various suspension flow rates. The fraction that is active is seen to increase to a maximum in the tuning heating-rate range and decrease to zero above this window. As with c_s, the maximum value of F is seen to depend on the suspension flow rate and heating rate, which in turn will change as the other loop conditions change. Also, it is seen that the $F_{\max}$ will not always equal the PCM charge in the suspension, F^*, and that if the suspension flow rate and heating rate are not appropriate for the other conditions, then only a portion of the PCM load will be active. For example, for the case of 0.004-kg/s flow the heat transfer coefficients in the loop are such that the minimum ΔT occurs at approximately 90 W. This heating rate, however, is not sufficient to fully utilize all the PCM at 0.004 kg/s, and hence F is only approximately 11% when F^* is 17.5%. Thus MEPCM capsules are being circulated that are not necessary and that cannot be utilized in the thermal balance. At the lower flow rates, F becomes equal to its maximum possible value, F^*, and all of the PCM is being utilized.

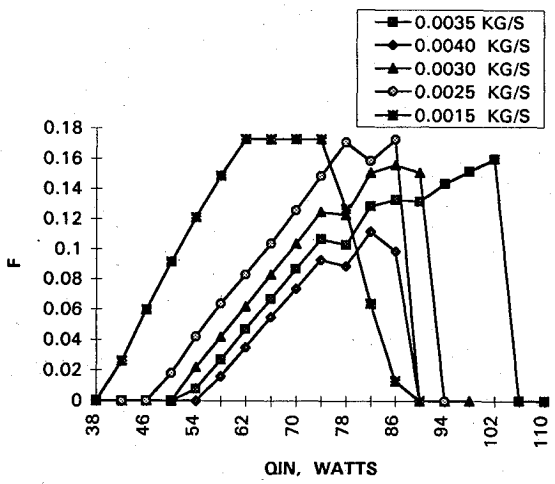

Fig. 5 Simulated variation of active phase-change fraction as heating rate varies.

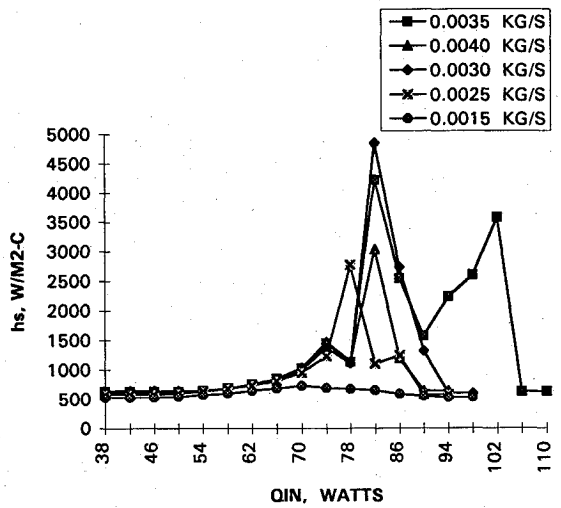

Fig. 6 Predicted variation of average convective heat transfer coefficient with system heating rate.

The heat transfer coefficient of the suspension flow is calculated in the simulation by using a fundamental relationship between Nu, Re, Pr, and tube L/D. That is, a relationship such as $Nu = f(Re\,Pr, L/D)$ [Eqs. (10) and (11)] should apply as long as the fluid is a continuum, is Newtonian, and has properties sufficiently uniform over the flow area. The last condition, of course, is not strictly met by an MEPCM suspension. Nevertheless, in the simulation it is assumed that on an overall average basis for the heat exchanger the same relationship applies and that the properties are determined on an effective basis, which includes latent effects. Hence, c_s directly influences Pr_s and therefore Nu and h_S. By utilizing a c_s corresponding to the tuning window and perhaps of the order of 100, as compared to a $\bar{c}$ of unity for sensible circumstances, it is clear that h_S will compute to be a much greater number. Figure 6 illustrates the suspension heat transfer coefficient computed in the simulation and the enhancement that occurs when c_s is enhanced by the latent effects. This phenomenon is also responsible for the reductions in surface temperatures in the tuning zone, which were seen in the simulations as well as in experiments.

A set of experiments were carried out explicitly to test the assumptions and methodology utilized to evaluate the heat transfer coefficient in the simulation. The test matrix included pure water as the working fluid as well as five suspensions: 23% octadecane (OCTA230), 26% octadecane (OCTA260), 27.2% octadecane (OCTA272), 32% eicosane (EIC320), and 32.6% eicosane (EIC326). Each fluid was circulated in the loop as it was powered up through the heat range of 10 to approximately 100 W. All other conditions were maintained the same. At each test point the flow capacity was evaluated by multiplying the suspension flow rate by its effective specific heat. The heat transfer coefficient was determined

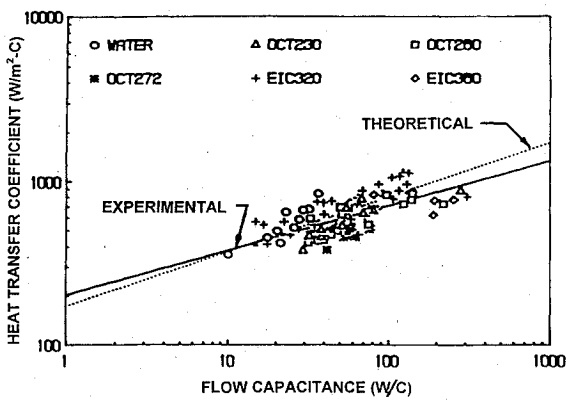

Fig. 7 Average heat transfer coefficient vs flow capacity for water and all suspensions tested.

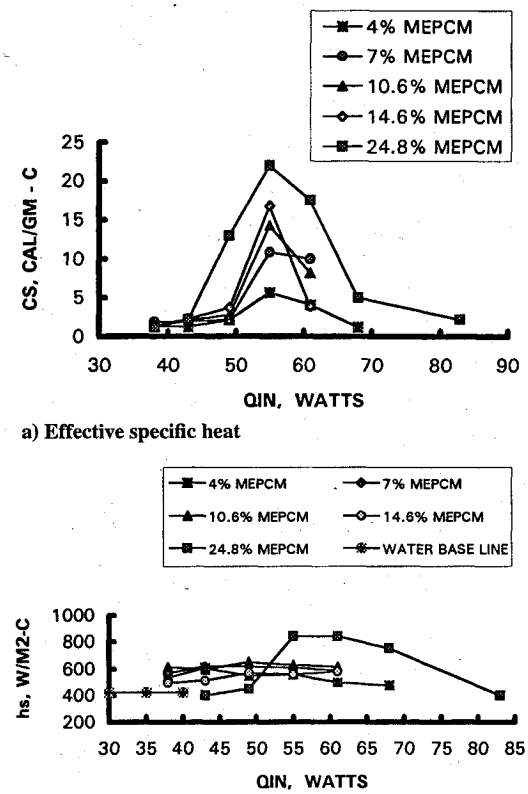

Fig. 8 Experimental variation of effective specific heat and heat transfer coefficient for various MEPCM concentrations of heptadecane in water (22.5°C melting temperature).

by averaging seven wall temperature measurements and averaging the inlet and outlet bulk temperature of the working fluid, and calculating h_S as $Q_{\text{in}}/A_S(\bar{T}_S - \bar{T}_f)$. These data are seen in Fig. 6, a total of 131 data points taken for the six working fluids. A statistical analysis of the data[14] indicated the following relationship:

$$h_S = 245(\dot{m}_s c_s)^{0.23} \tag{18}$$

with a standard error of estimate of 12%, a correlation coefficient of 0.99, and a 95% confidence level. The classical Sieder–Tate expression predicts

$$h_S = 172(\dot{m}_s c_s)^{0.33} \tag{19}$$

Both expressions are shown in Fig. 7 with the data. It is very clear that the classical expressions for heat transfer are entirely adequate if the properties are made to include latent effects and the system is well balanced (tuned). The differences are seen to be well within experimental error in the heating-rate range of practical interest.

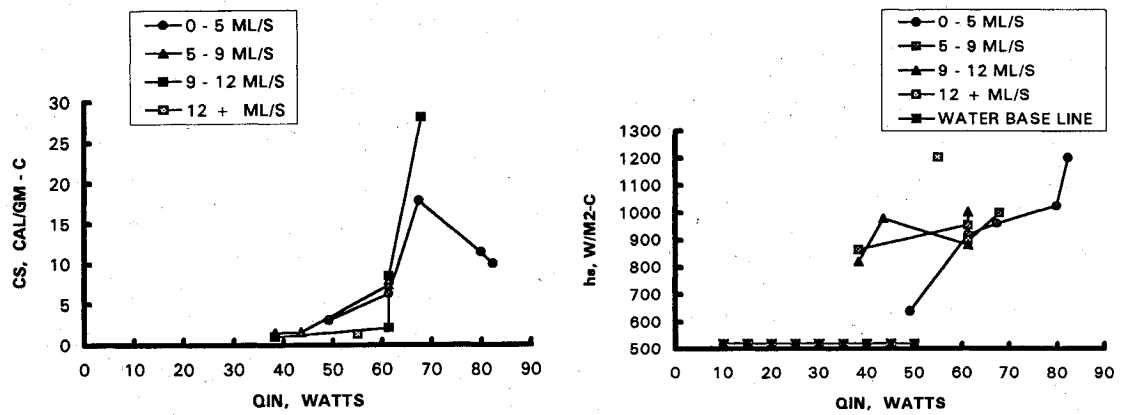

a) Effective specific heat b) Heat transfer coefficient

Fig. 9 Experimental variation of effective specific heat and heat transfer coefficient of octadecane in water (27°C melting temperature).

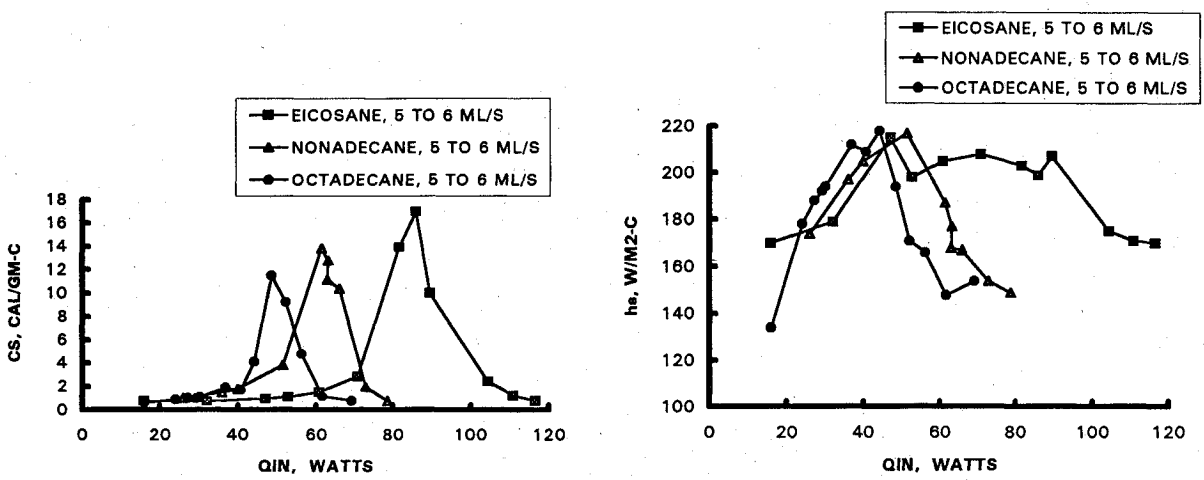

a) Effective specific heat b) Heat transfer coefficient

Fig. 10 Experimental variation of effective specific heat and heat transfer coefficient of several MEPCM materials in silicone oil: octadecane (27°C), nonadecane (32°C), and eicosane (37°C).

This result is extremely important because it provides a confirmation of a straightforward (although iterative) technique of carrying out system simulation.

In addition to the experiments carried out to explicitly confirm the heat transfer methodology described above, several additional sets of experiments were carried out. Figure 8 is a summary of data taken from experiments with heptadecane in water at various concentrations of microcapsules. These data have an uncertainty of approximately 12%, as before. The general trends of the data are seen to largely confirm those of the simulation predictions, although with some differences due to the inability of the experimental apparatus to exactly match the simulation conditions. The tuning window is centered at approximately 55 to 60 W, slightly lower than the 80 W predicted, but well within the uncertainty of the simulation. The discrepancy is believed to be due to the assumption that the melting and freezing temperatures of the PCM are equal. In experiments these were found to be somewhat different, depending upon the conditions. The effective specific heat is seen to improve somewhat even with a small amount of the PCM in the fluid, but the full improvement is not realized until the maximum load of approximately 25% is tested. Loads greater than this are not practical, because of the increased viscosity and pumping power required. The heat transfer coefficient is seen to improve significantly at the higher concentration but is not improved much at the lower concentrations. This was expected, since the effective specific heat is much more sensitive to the latent effects than is the heat transfer coefficient.

Tests of octadecane in water were also carried out, as shown in Fig. 9. Since octadecane melts at a higher temperature (27°C, as compared to 23°C for the heptadecane), more heat was required and higher loop temperatures. These suspensions were approximately 25% by capsule weight and are seen to clearly show specific heat improvement and enhancement of the heat transfer coefficient.

A series of tests were carried out to explore the potential of the MEPCM fluid's applicability to electronic and avionic cooling—that is, the behavior of suspensions made of MEPCM capsules and dielectric fluids. Here suspensions were constructed of eicosane, nonadecane, and octadecane in Dow Corning silicone oil (5 cS). Figure 10 illustrates the very sharp and pronounced improvement achieved in the specific heat, as well as the very significant improvement in heat transfer coefficient. Surface temperatures were very well moderated by the PCM, and the solvent nature of the silicone oil seemed to have no effect on the MEPCM capsules.

Conclusions

During the work, octadecane, eicosane, heptadecane, and nonadecane were all microencapsulated successfully, pumped in a liquid-coupled heat exchange loop, and shown to reduce system temperatures and to increase effective specific heats and heat transfer coefficients. It was shown that the improvements in the thermal performance of such a loop depends upon the system conditions of coolant flow rate and temperature, heat exchanger design factors, and the MEPCM fluid flow rate. These tuning conditions were also shown to be predictable by system analysis techniques if heat transfer modeling techniques are employed that utilize effective properties and iterative analyses.

Acknowledgments

This work was sponsored by NASA and the U.S. Air Force Wright Research Development Center under Contracts NAS8-35840, NAS9-17952, and F33615-86-C-3430.

References

[1]Lane, G. A., and Glew, D. N., "Heat-of-Fusion Systems for Solar Energy Storage," *Proceedings of Workshop on Solar Energy Storage Subsystems for the Heating and Cooling of Buildings* (Charlottesville, VA), edited by L. U. Lilleleht, National Science Foundation, NSF RAN 75-041, 1975, pp. 43–55.

[2]Mehalick, E. M., and Tweedie, A. T., "Two Component Thermal Energy Storage Material Program Phase I Final Report," General Electric Co., DOE Rept. EY-76-02-2845, Philadelphia, PA, Feb. 1979.

[3]Hendel, F. J., and Mulligan, J. C., "Refrigeration in Space by the Fluidized Technique," *Journal of Spacecraft and Rockets*, Vol. 2, No. 4, 1965, pp. 616–618.

[4]Hart, R., and Thornton, F., "Microencapsulation of Phase Change Materials," Capsulated Systems, Inc., Final Rept. to Ohio Dept. of Energy, Contract 82-80, Fairborn, OH, Dec. 1982.

[5]Kasza, K. E., and Chen, M. M., "Improvement of the Performance of Solar Energy of Waste Heat Utilization Systems Using Phase Change Slurry as Enhanced Heat Transfer Storage Fluid," *Journal of Solar Energy Engineering*, Vol. 107, Aug. 1985, pp. 229–236.

[6]Charunyakorn, P., Sengupta, S., and Roy, S. K., "Forced Convection Heat Transfer in Microencapsulated Phase Change Material Suspensions: Flow in Circular Ducts," *International Journal of Heat and Mass Transfer*, Vol. 34, No. 3, 1991, pp. 819–835.

[7]Colvin, D. P., Mulligan, J. C., Bryant, Y. G., and Duncan, J. D., "Microencapsulated Phase Change Material Heat Transfer Systems," Flight Dynamics Lab., U.S. Air Force Wright Research and Development Center, Rept. WRDC-TR-89-3072, Aug. 1989.

[8]Colvin, D. P., Mulligan, J. C., Bryant, Y. G., Duncan, J. D., and Gravely, B. G., "Microencapsulated PCM Suspensions for Heat Transfer and Energy Storage in Spacecraft Systems," *Sixth Symposium on Space Nuclear Power Systems* (Albuquerque, NM), Vol. 2, edited by M. S. El-Genk and M. D. Hoover, 1989, Orbit, Malabar, FL, pp. 303–306.

[9]Colvin, D. P., Mulligan, J. C., and Bryant, Y. G., "Enhanced Heat Transport in Environmental Systems Using Microencapsulated Phase Change Materials," Society of Automotive Engineers, Paper 921224, July 1992.

[10]Sohn, C. W., and Chen, M. M., "Microconvective Thermal Conductivity in Disperse Two-Phase Mixtures as Observed in a Low Velocity Couette Flow Experiment," *Journal of Heat Transfer*, Vol. 103, No. 1, 1981, pp. 47–51.

[11]Watkins, R. W., Robertson, C. R., and Acrivos, A., "Entrance Region Heat Transfer in Flowing Suspensions," *International Journal of Heat and Mass Transfer*, Vol. 19, No. 6, 1976, pp. 693–695.

[12]12. Vand, V., "Theory of Viscosity of Concentrated Suspensions," *Nature*, Vol. 155, No. 3934, 1945, pp. 364–365.

[13]Torquato, S., "Bounds on the Permeability of a Random Array of Penetrable Spheres," *Physics of Fluids*, Vol. 30, No. 3, 1986, pp. 633–641.

[14]Romesburg, L. J., "Enhancement of Heat Transfer in Liquids with Microencapsulated Phase-Change Materials," M.S. Thesis, Dept. of Mechanical and Aerospace Engineering, North Carolina State Univ., May 1988.

R. K. Clark
Associate Editor